


Jana Publication & Research

Morphotectonic analysis by coupling a digital terrain model (DEM), radar data (Sentinel-1C) and field data from the Easter...

 12

 BioTech

 Institut Seni Indonesia Surakarta

Document Details

Submission ID

trn:oid::1:3169692040

Submission Date

Mar 1, 2025, 12:48 PM GMT+7

Download Date

Mar 1, 2025, 4:04 PM GMT+7

File Name

IJAR-50450.docx

File Size

5.2 MB

17 Pages

4,440 Words

25,896 Characters





9% Overall Similarity

The combined total of all matches, including overlapping sources, for each database.




Filtered from the Report

- ▶ Bibliography
- ▶ Quoted Text

Match Groups

-  **13 Not Cited or Quoted 4%**
Matches with neither in-text citation nor quotation marks
-  **16 Missing Quotations 4%**
Matches that are still very similar to source material
-  **0 Missing Citation 0%**
Matches that have quotation marks, but no in-text citation
-  **0 Cited and Quoted 0%**
Matches with in-text citation present, but no quotation marks

Top Sources

- 7%  Internet sources
- 8%  Publications
- 0%  Submitted works (Student Papers)

Match Groups

- 13 Not Cited or Quoted 4%**
Matches with neither in-text citation nor quotation marks
- 16 Missing Quotations 4%**
Matches that are still very similar to source material
- 0 Missing Citation 0%**
Matches that have quotation marks, but no in-text citation
- 0 Cited and Quoted 0%**
Matches with in-text citation present, but no quotation marks

Top Sources

- 7% Internet sources
- 8% Publications
- 0% Submitted works (Student Papers)

Top Sources

The sources with the highest number of matches within the submission. Overlapping sources will not be displayed.

| | | | |
|-----------|----------------|---|-----|
| 1 | Internet | www.ej-geo.org | 2% |
| 2 | Publication | J.G. Shellnutt, H.T. Tran, T.-Y. Lee, M.-W. Yeh, R.B.-J. Hsieh, H.-Y. Lee. "Late Neoprot... | <1% |
| 3 | Internet | hdl.handle.net | <1% |
| 4 | Publication | Felix Djerosseem, Armin Zeh, Moussa Isseini, Olivier Vanderhaeghe, Julien Berger, ... | <1% |
| 5 | Internet | hal.archives-ouvertes.fr | <1% |
| 6 | Internet | researchers.uss.cl | <1% |
| 7 | Student papers | Flinders University | <1% |
| 8 | Publication | Mahir Mahmod Hason, Malik R. Abbas, Baharin Bin Ahmad, Talib R. Abbas. "Monit... | <1% |
| 9 | Publication | Noudiédié Kamgang Julie Agathe, Tcheumenak Kouémo Jules, Fozing Eric Martial,... | <1% |
| 10 | Publication | Errami Maryam, Algouti Ahmed, Algouti Abdellah, Farah Abdelouhed. "Mapping a... | <1% |

| | | | |
|----|-------------|---|-----|
| 11 | Internet | epe.lac-bac.gc.ca | <1% |
| 12 | Internet | repository.up.ac.za | <1% |
| 13 | Publication | "Remote Sensing and Water Resources", Springer Science and Business Media LL... | <1% |
| 14 | Publication | Geology and Resource Potential of the Congo Basin, 2015. | <1% |
| 15 | Publication | Oumarou Faarouk Nkouandou, Jacques-Marie Bardintzeff, Aminatou Fagny Mefir... | <1% |
| 16 | Internet | dicames.online | <1% |
| 17 | Internet | publikationen.bibliothek.kit.edu | <1% |
| 18 | Internet | scirp.org | <1% |
| 19 | Internet | www.geokniga.org | <1% |
| 20 | Publication | Jean Marcel Abate Essi, Jean Marcel, Diab Ahmad Diab, Joseph Quentin Yene Atan... | <1% |
| 21 | Publication | Mohamed Abd El-Wahed, Mohamed Attia. " Structural and tectonic evolution of s... | <1% |

Morphotectonic analysis by coupling a digital terrain model (DEM), radar data (Sentinel-1C) and field data from the Eastern part of the Ouaddaï massif (Eastern Chad)

Summary

8 The study area lies between latitudes 13°15' and 13°45' North and between longitudes 21°24' and 22°2' East. Administratively, it is located in the department of Asougha, province of Ouaddai. The aim of this work was to carry out a morphotectonic analysis by coupling a digital terrain model, radar data and field data. We used SRTM images, Sentinel 1-C radar and field campaigns. The satellite images were analysed using cartographic software (ArcGIS, SNAP, Geomatica PC, RockWork, Global Mapper, Surfer) and Stéronet. Observations from the 3D map were used to divide the study area into three morphological units: Unit I, the lowest (altitude < 700m) where the watercourses are located; it is made up of plains and valleys. Unit II, the largest, has a medium to high altitude (700-900m). This geomorphological unit is made up of hills and plateaux; and Unit III is that whose altitude is > 900m. This unit is made up of circumscribed hills and mountain ranges. The lineaments obtained from Sentinel -C radar gave two main fracture directions: ESE-WNW and SE-NW. Field data provided the lithological type, mainly granitoids. These granitoids are fractured almost everywhere in the study area. These fractures follow the directions of their host rocks.

20 **Keywords:** Ouaddaï Massif, geological mapping, Lineament, Teledetection, Morphotectonics, radar

Introduction

11 Chad is part of the Central African orogenic belt, formed during the Neoproterozoic (Isseini, 2011); (Bessoles, B. & Trompette, 1980). This orogenic belt remains the last tectonic event. The result of this event is the formation of five major mountain ranges of Pan-African age, with a mainly granitic basement interspersed with metamorphic formations (Kusnir, 1995). Alongside this basement are volcanics and surface and groundwater resources. The basement is covered by overburden formations (approximately 85% of Chad's total surface area) made up of two major sedimentary basins: the Erdis basin in the north, which accounts for most of the surface area, and the Lake Chad basin, located throughout the southern and central parts of the country (Schneider-J.L and Wolff, 1992; B.R.G.M, 2010b). Basement zones and sedimentary basins are rich in mineral resources (Chaussier, 1970; B.R.G.M, 2010a; World bank group, 2023).

5 In this work, we review the literature on basement zones and their associated mineralization.

1- Geological context

Studies into the geology of Chad began in the colonial years (around 1900). Research increased after 1945. We might mention the work of Garde, 1911 on the Kanem; Tiho, 1913; Lacroix, 1919 on the Bourkou Ennedi Tibesti; Cartier, Grossard, Fenayer and Fritel (1924-1925) on the Ouadda; Babet,

6 1940 on the Chari-Baguirmi; Van Aubel, 1942 on the Mayo-Kebbi. Unfortunately, these data are not currently available in the archives. Work intensified around 1990, leading to the production of several maps (sheets) by the Central African Mining and Geology Directorate, the Bureau de Recherche Géologique et Minière (B.R.G.M) and the Institut Equatorial de Recherches Géologiques et Minières. These include: (Bessoles, B. & Trompette, 1980; Chaussier, 1970; Gsell, J. and Sonnet, 1962; Gsell J and Sonnet J., 1960; J, 1960; Mestraud, 1964; Pias, 1964; Wolff, 1964). Most of these offices have carried out reconnaissance mapping of the various geological formations in Chad. On the basis of these data, the lithostratigraphy of the geological formations of Chad can be divided into: neoproterozoic granitoids, crystallophyll formations, paleozoic cover formations or sediments and volcanics (Wolff, 1964).

13 2 Following this work, further work was carried out within the framework of international correlation on stratigraphy or lithostratigraphy ((Kasser, 1995); (Penaye et al., 2006). This work led to the definition and identification of the major lithological structures in the Mayo-kebbi massif, the Tibesti massif to the north, the Ouaddaï massif to the east, the central massif, which extends the Ouaddaï massif to the west, and the Mbaibokoum massif to the south (Kasser, 1995).

3 2 More recent work has been carried out, especially in the context of training for trainers. Examples include work carried out in the Mayo-kebbi massif (Mbaguedje, 2015); (Isseini, 2011); (Doumnang, 2006); and in the Mbaibokoum massif (Mbaitoudji, 1984). Other more recent work has been carried out as part of university studies or mining research. These include work carried out in the Tibesti massif (Doumnang et al., 2024); in the Ouaddaï massif (Djerossem Nenadji, 2018; Djerossem et al., 2020, 2024; Malik et al., 2024); (Hingue et al., 2024, 2025); (Malik et al., 2024); (De Wit et al., 2021); or in the Central massif (Shellnutt et al., 2017, 2018, 2020). Most of these studies describe the crystalline massifs of Chad as being mainly granitic.

17 21 The Ouaddaï massif is located in the southern part of the metacraton (Abdelsalam et al., 2002, 1998, 2011; Abdelsalam & Stern, 1996; Elsheikh et al., 2011; Ibinoof et al., 2016, 2021; Liégeois et al., 2013; Stern & Abdelsalam, 1998). It has the shape of a plateau and covers more than 500 km². They outcrop from the border with the Tibesti massif, mainly in its southern part (to the north, the Ennedi). To the east, it extends into Darfur in Sudan. In the west, the Ouaddaï massif is bordered by the Central massif (Schneider, 2001).

4 In lithostratigraphic terms, the Ouaddaï massif is mainly granitic. However, in its southern part, metamorphic formations outcrop in abundance (Gsell J and Sonnet J., 1960; Gsell, J. and Sonnet, 1962; Pias, 1964; Wolff, 1964; Kusnir, 1989, 1995).

4 On the lithostructural basis, (Gsell J and Sonnet J., 1960; Gsell, J. and Sonnet, 1962) describe the Ouaddaï massif as : (i) metasedimentary and metavolcanic rocks (quartzite schist, marble, cipolin, migmatite); (ii) rocks with little or no metamorphism (migmatite, anatexis granodiorite, anatexis

1 granite); (iii) post-tectonic plutonic formations (calc-alkaline granite with two micas, alkaline granite, porphyroid calc-alkaline granites with biotite and amphibole, granulites, aplitic granites, microdiorites, syenites, diorites, microgranites, basalts); (iv) eruptive rocks and various plutonic rocks of intermediate to felsic composition, forming plutons and veins intersecting the metamorphic rocks (Fig. 1).

14 The work of (Kusnir, 1995) illustrates that the Ouaddaï massif is purely granitic and migmatitic. The metamorphic rocks identified consist of : (1) graphitic schists associated with micaceous quartzites and amphibolites, located near Waya Waya, to the north-west of Guéréda; (2) banded ferruginous quartzites (Hadjer Hadid to the south-west of Adré); (3) highly bedded fine-grained amphibole gneisses forming elongated reliefs in a migmatitic zone (about 50 km to the north-east of Iriba) ; (4) migmatites and embréchites, which form the main formations in the region near the Sudanese border; (6) to the west of Mourah, cordierite and sillimanite anatexites appear in a diffuse zone within the migmatitic granite; (7) meta-ultrabasites, which are less rich and include pyroxenites, which form numerous outcrops between Adré and Am Leiouna. Massive amphibolites outcrop in several places (to the north and north-west of Guereda, at the foot of the Modoina sandstone cliff). More recently, the geological formations to the east of the Ouaddai massif have been mapped as : (1) migmatites, on the Hadjer-Hadid axis; Farchana-Abou goulam-Molou-Biské; (2) calc-alkaline granite around Abougoulem and north of Hadjer-hadid; (3) granite around Abéché, at Molou ; (4) calc-alkaline granite with porphyritic facies south-east of the village of Kadigué, around 14 km east of Molou; (5) calc-alkaline granite around Abéché, west of Hadjer-hadid, at Abou goulem (B. R.G.M, 2010b); (Hingue et al., 2024, 2025). All these rocks are Neoproterozoic in age. In the vicinity of Iriba, the geological formations are mapped as basanites with a SiO₂ content of around 41-45%. These basanites are described as an extension of the Cameroon volcanic line, located to the west and south of Cameroon (F. N. Djerosse et al., 2024).

1 In the Am Zoer sector, the rocks are mainly migmatitic and more or less differentiated (SiO₂=55.8 to 74.70%), calc-alkaline, metaluminous to peraluminous. They are predominantly type I granites (A/CNK<1.1) with the exception of mylonite and migmatite, which belong to type S granites (Pazeu, 2018); dated by U/Pb on zircon, the granitoids give Pan-African ages (620-585Ma (Alexis et al., 2019).

Towards the south of the massif, metamorphic rocks outcrop very widely (Michael, 2017); (Mbaiade, 2023). These are metasedimentary rocks, mainly of Neoproterozoic age (amphibolites, cipolins, gneisses, micaschists, micaceous quartzites, metapelites, schists and marbles), amphibolites and basalts interbedded with S-type leucogranites dated at 635Ma ±3 and 612 Ma± 8 by U-Pb on zircon; type-I granitoids of Pan-African age (538±5Ma on zircon), (Djerosse, 2018).

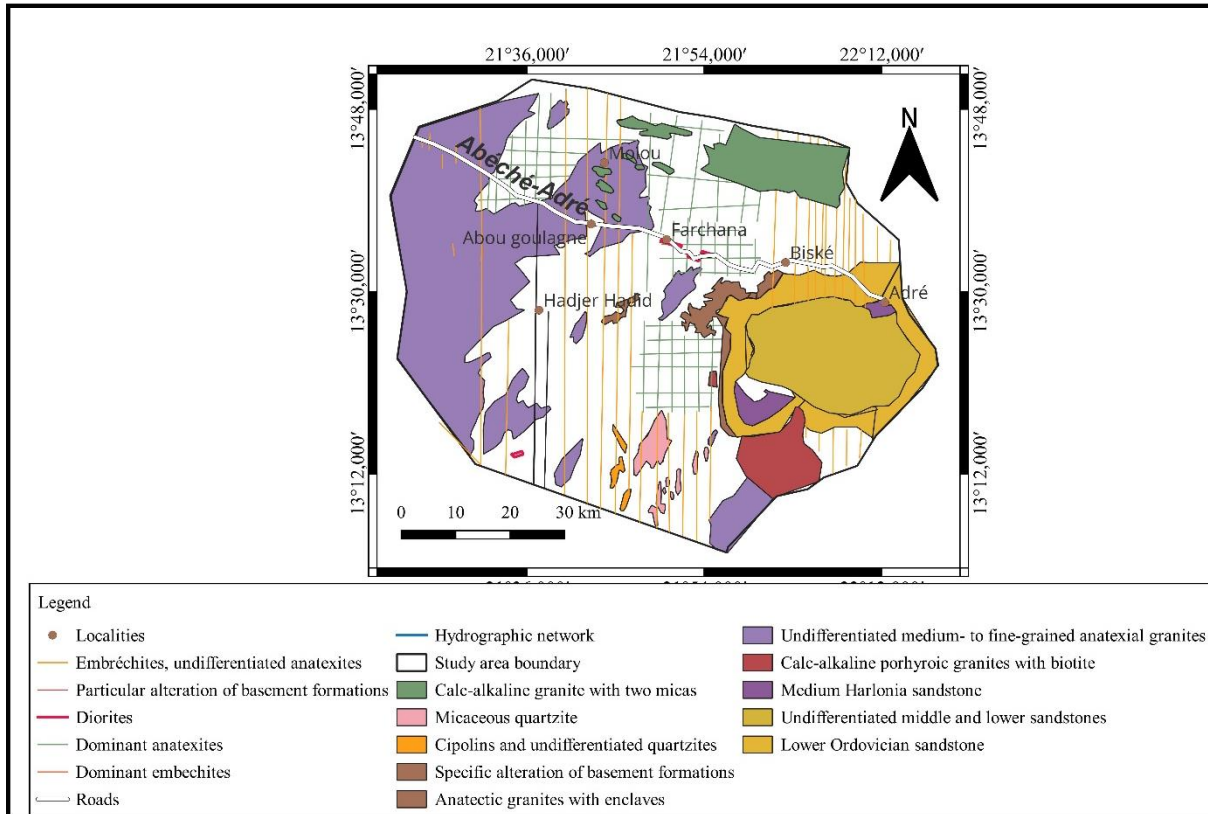


Figure 1: Reconnaissance geological map of the Adré sheet, scale 1:500,000, adapted from (Gsell J and Sonnet J., 1960).

2- Materials and methods

Four types of data are used in this article: the digital terrain model, radar (Sentinel-1C), bibliographic data and field data.

The digital terrain model generated from the SRTM image extracted using Global mapper and Arcgis is used to provide an overall morphological view of the massif and to generate several thematic maps (3D map, topographical profile map, etc.). The Sentinel1-C radar was used to extract the lineaments in SNAP, Geomatica PC and the steering rosette in Arcgis and Rockwoks 17. The polarisation used is called cross-polarisation (horizontal-vertical polarisation). The various steps used in this work are summarised in Figure 2.

The bibliographic data consisted of articles, doctoral theses, master's theses, books and reviews:

- 1. ■ a geological reconnaissance map of Adré at a scale of 1:500,000. This map was published by the Institut Equatorial des Recherches et d'Etudes Géologiques et Minières by Gsell and Sonet, 1960, based on a 1/200,000 scale photograph from the Institut Géographique National. It was used to identify geological formations and locate structural features;
- Vector data (shapefiles). The vector data consists of the administrative boundaries of the study area, localities, watercourses and roads.

Terrain data consists mainly of geological structures (fracturing, foliation) and lithologies. This data was obtained during various field campaigns. This data is analysed using Stéronet software and analysed in the form of a directional rosette. This field data is used to validate the lineament and digital terrain model data and to better interpret the geological structures in the study area.

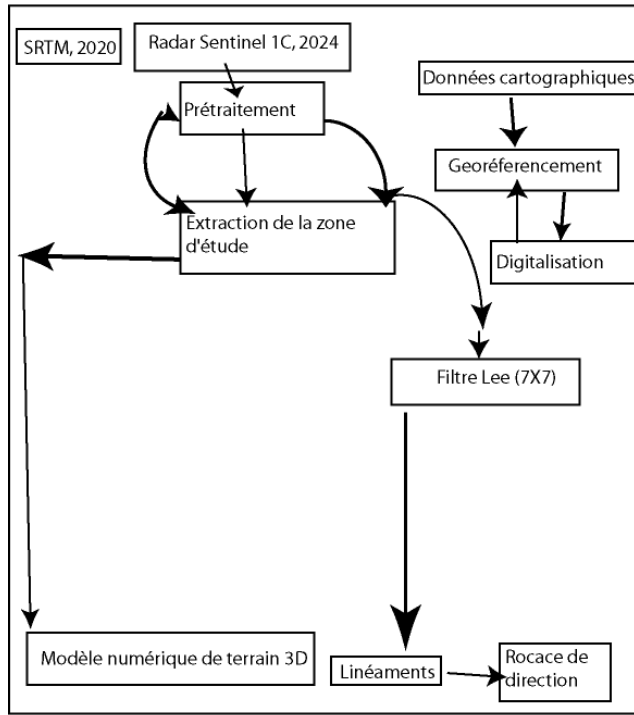


Figure 2: image processing stages using the software

3- Results

a- Contribution of remote sensing to geological and structural mapping

Remote sensing has become a modern, effective tool for mapping geological and structural formations with a high degree of accuracy (Scanvic, 1986).

Orography

The orography of the study area is divided into four geomorphological units (units I, II and III).

Unit I comprises the lowest relief. It includes landforms at altitudes of $\leq 700\text{m}$ (Fig.3). It corresponds to the Ouadi Hamra depression and isolated flood plains in several places.

Unit (II) consists of the intermediate relief (700-900 m). This is the largest geomorphological unit. It comprises moderate to high relief. The slopes in this unit are moderate to steep (Fig. 4).

Unit (III) has an altitude $>900\text{m}$. It characterises the mountains to the east of Abougoulem, to the north of Hadjer-hadid and to the north-east of Molou. It has steep slopes (Fig.4).

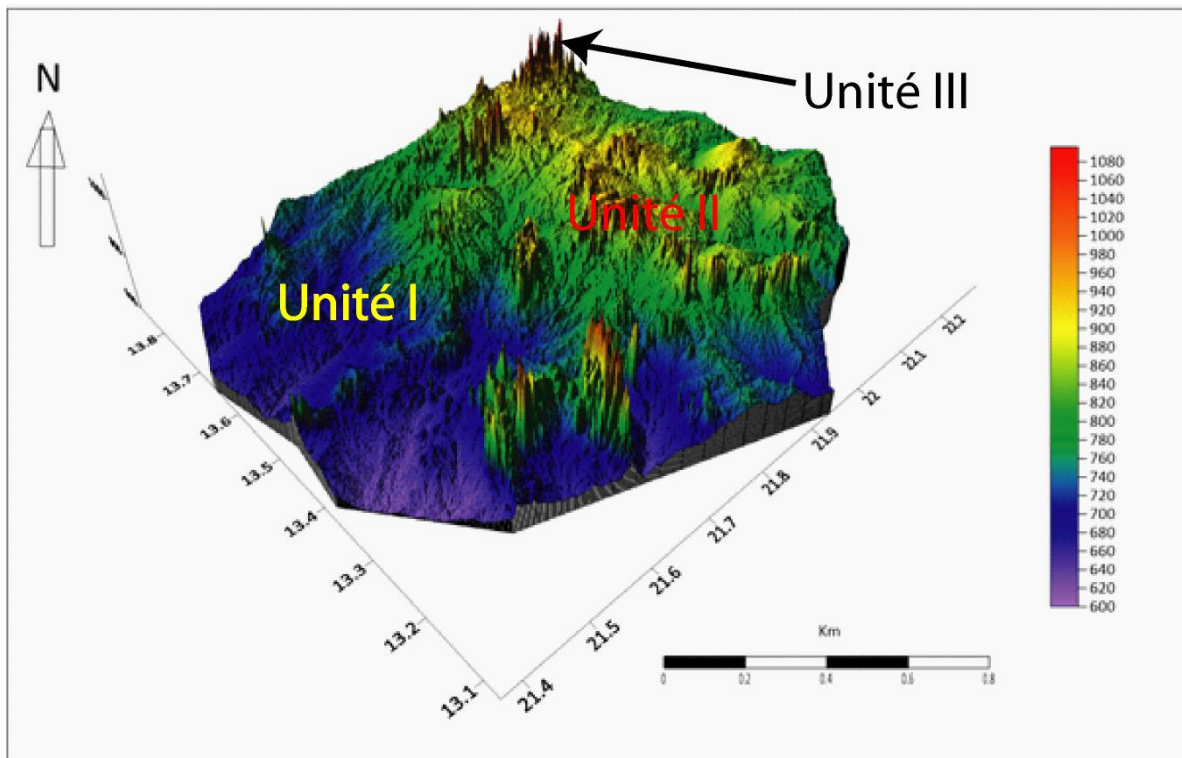


Figure 3: 3D digital terrain model.

Relief typology

7 The orographic units (I) are those that drain the watercourses. They are located mainly to the north-east and south of the study area. They follow a NE-SW alignment. This unit is controlled by the Ouaddaï Hamra valley and the Bitéa streams, a tributary of the Batha (Fig. 4).

Geomorphological Unit II consists of hills forming mountain ranges from the north of the town of Hadjer-hadid to the south of the village of Abougoulem. This range is oriented SW-NE. Other mountain ranges can be seen to the north of the village of Molou, and to the east of the town of Farchana, specifically to the west of Biské, where it forms hills in several places.

Unit III is the largest, and is dominated by medium-altitude hills (Hadjer-hadid

Unit IV corresponds to the high altitude areas. It is defined by hills oriented SW-NE.

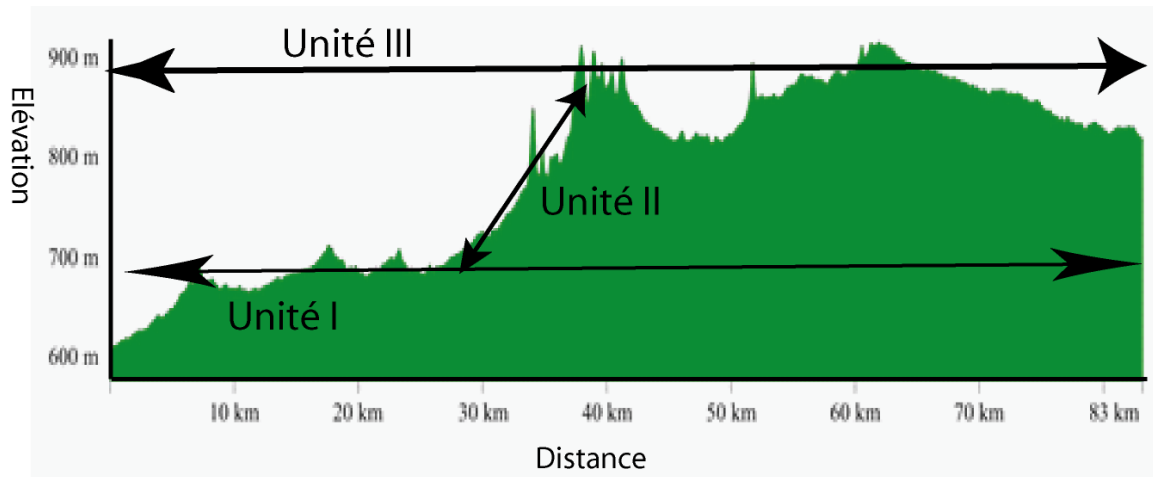


Figure 4: Topographical profile showing the different altitudes and slopes of the study area

Lineament mapping

Lineaments symbolise linear geological objects, arrays of geological objects (faults, joints, schistosity) that are fairly close together, geomorphological discontinuities, (Faure, 2001); (Théodore et al., 2012). These are structural faults of variable length (Faure, 2001); (Richards, 2000). The lineaments extracted from Sentinel 1-C radar were used to produce the lineament map. A total of 1096 lineaments were detected and extracted (Fig.5). They are unevenly

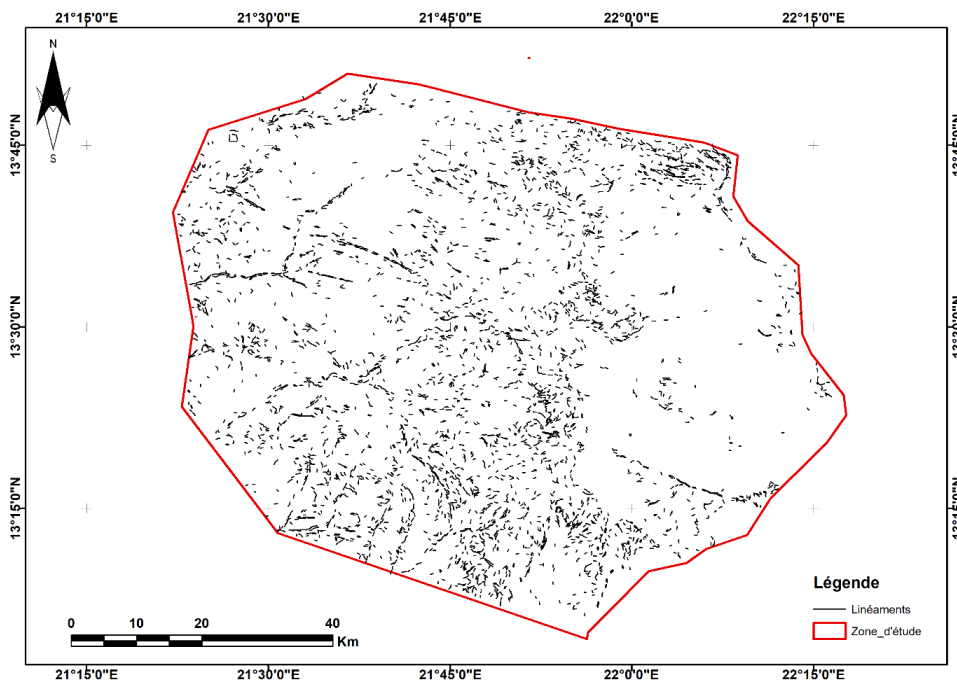


Figure 5: Lineament map extracted from Sentinel -1C RADAR images.

Directional rosette

The directional rosette shows a spread of lineaments in all directions (Fig. 6). However, certain lineament directions stand out. These are ESE-WNW (90° to 115°), SE-NW (45° to 65°), ESE-WNW and SSE-NNW (165° to 180°). Two of these directions are the main ones. These are: the SE-NW direction (115° to 160°), and the ESE-WNW direction (90° to 115°) and (135° to 160°).

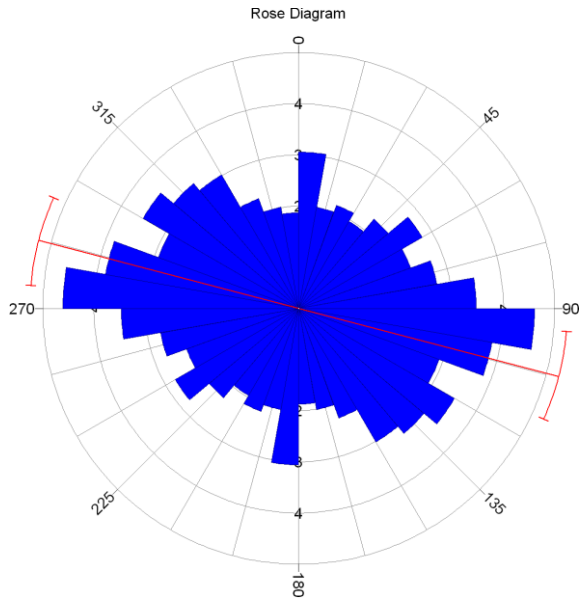


Figure 6: Directional rosette extracted from Sentinel-1C Radar images

The density of lineaments is mainly located in geomorphological units III and IV (to the south-west, south-east and north of the study area. to the north-east and south of the study area. They are oriented parallel to the hydrographic network and the relief. This orientation would suggest a tectonic (geological) origin.

b- Field data contribution

Lithology

On a landscape scale, the geological formations to the east of the Ouaddai massif (Adré group) outcrop as slabs, blocks and domes, or even mountain ranges. At the outcrop and rock scale, they are arranged metrically, decametrically and even kilometre-wise (Fig. 7).



Figure 7: Photograph of the formations in the study area. a) Panoramic view of the diorites at Farchana; b) Blocky outcrop of the granodiorites at Hadjer-hadid; c) Foliation in the granodiorites at Hadjer-hadid; and d) Fracturing of the alkaline granites at Farchana.

The lithology of the study area consists purely of granitoids (biotite and amphibole granite, alkaline granite, granodiorite, diorite, anatexis granite).

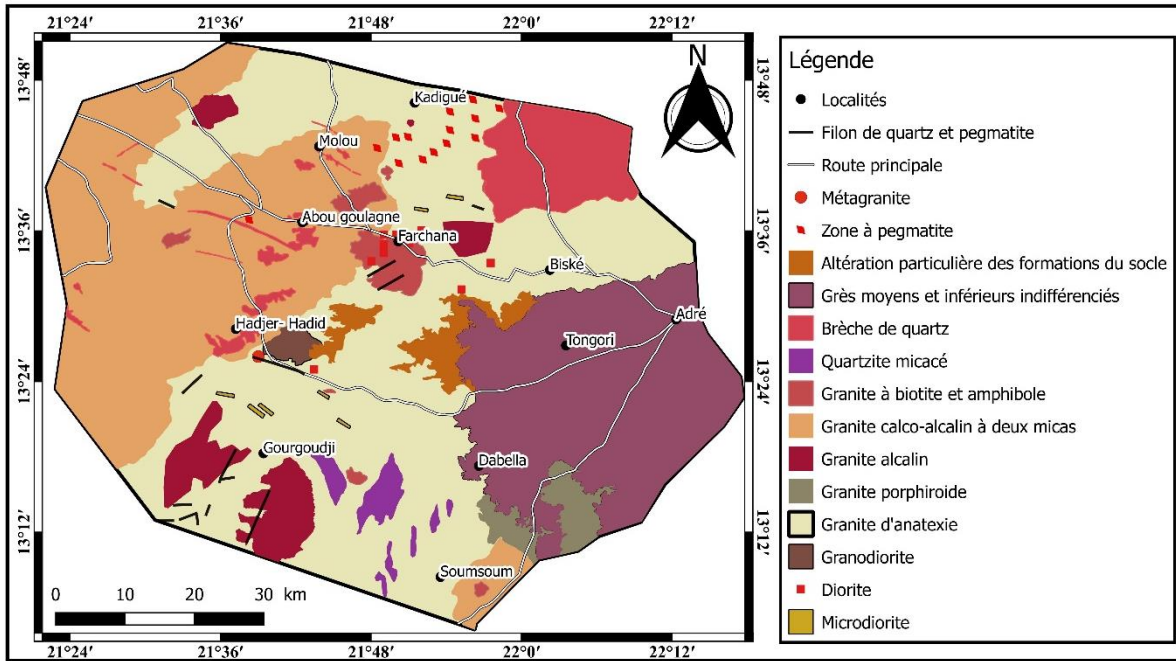


Figure 8: Segment of the geological map of the eastern Ouaddaï massif

Tectonics

18

The study area is made up of rocks with little or no deformation. Nevertheless, a number of structures have been identified and described.

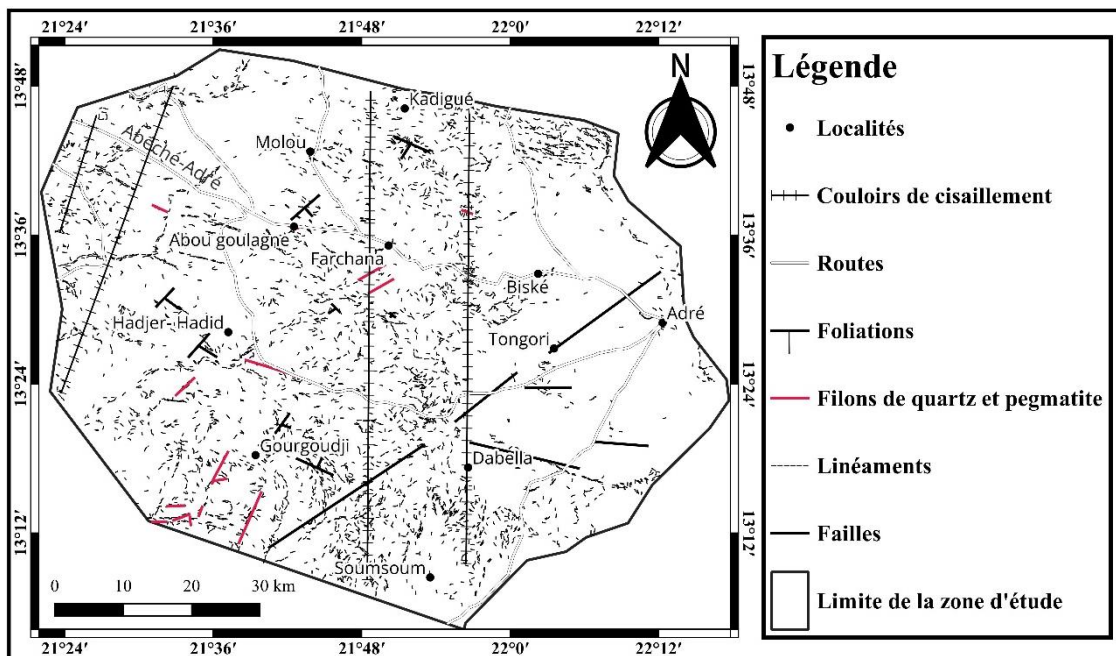
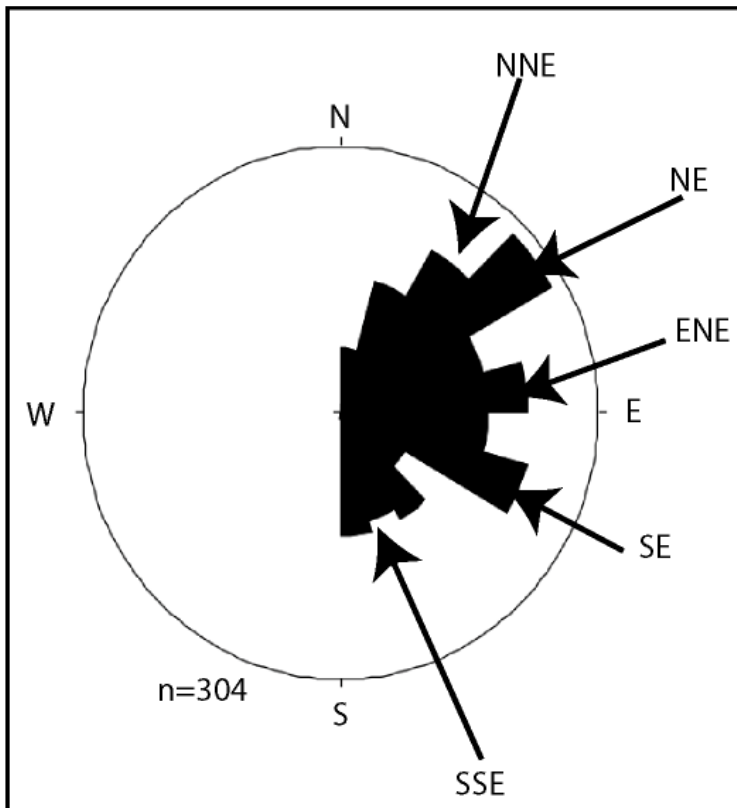


Figure 9: Structural segment of the Eastern Ouaddaï massif.

19 The foliation observed is magmatic (Fig. 9). This foliation is observed in granodiorites, biotite and amphibole granites and alkaline granites. This is the first phase of deformation observed in the study area.

Veins are found throughout the study area. Pegmatite veins are found throughout the lithologies (Fig.9). They are mapped in abundance in the kadigué anatexis granites to the north-east of Molou, where they form SW-NE trending foci.

All the fracturing data thus obtained were used to produce the directional rosette (Fig.10). There are two main directions in this rosette: NE-SW and ESE-WNW.



10 Figure 10: Directional rosette of fractures in the study area.

4- Discussion

The topography of the study area is a plateau with a summit altitude of 110m. This altitude corresponds to the mountain ranges observed to the north-east of Molou and to the north of Hadjer Hadid.

a- Data control and validation

The control and validation of the lineament data enables the lineament data obtained to be validated against that obtained from the literature and field data (Scanvic, 1986).

b- Checking existing tectonic data in the study area

1 The lineaments mapped by Radar Sentinel 1-C yielded two main fracturing directions: ESE-WNW and SE-NW. These fracturing directions were also obtained by (Oussama, 2023); (Al-Djazouli et al., 2019). The geological map drawn up by (Gsell J and Sonnet J., 1960) (Schneider, 2001) also gives a similar fracturing direction. This direction corresponds to the main direction of the Precambrian basement of the Ouaddaï massif (B.R.G.M, 2010b; World bank group, 2023).

c- Checking DTM data against field data

5 The 3D DTM map obtained from the SRTM images was used to divide the morphology of the study area into map units: valleys, flat areas and hills (units I, II and III). On the ground, in the low-lying areas (unit I), the diorites are widely mapped. They follow the course of watercourses. Units II and III, mapped in the 3D DTM map as high-altitude areas, are mapped on the ground as circumscribed hills and mountain ranges with altitudes > 110m. These units are mapped precisely to the north-east of Molou and to the north of Hadjer-hadid. The hills are described as consisting mainly of biotite and amphibole granites, alkaline granites, anatexis granites, metagranites, quartz breccias and granodiorites. These results are confirmed in the work carried out by (Hingue et al., 2024, 2025).

Checking lineaments against field data

The validation of lineament data with that obtained in the field enables the physical recognition of lineaments mapped in the field, especially those of great importance in geology such as faults and shears. This technique is the most appropriate method for recognising lineaments. Over 300 fracture planes are measured in the field. The directional rosette obtained gave two main directions: ESE-WSW or N115°-135° and NE-SW or N45-70°. These latter directions are the same as those obtained from the Sentinel 1-C radar. This result corroborates those of (Hingue et al., 2025).

Conclusion

12 The morphotectonic study coupled with the DTM and radar data yielded three geomorphological units ranging from valleys to circumscribed hills. The lineaments obtained from Sentinel 1-C radar are those of geological origin and are oriented ESE-WNW and SE-NW. These directions also correspond to the direction of the different lithologies in the study area and follow the watercourse corridors. The field data thus obtained has enabled us to validate the various maps obtained from the radar images and the digital terrain model. It is now possible to map the geological structures using the radar digital terrain model and simply validate them with the field data.

Reference

Abdelsalam, G., M., Liégeois, Paul, J., Stern, & J., R. (2002). The Saharan Metacraton. *Journal of African Earth Sciences*, 34(3–4), 119–136. [https://doi.org/10.1016/S0899-5362\(02\)00013-1](https://doi.org/10.1016/S0899-5362(02)00013-1)

- Abdelsalam, M. G., Gao, S. S., & Liégeois, J. P. (2011). Upper mantle structure of the Saharan Metacraton. *Journal of African Earth Sciences*, 60(5), 328–336. <https://doi.org/10.1016/J.JAFREARSCI.2011.03.009>
- Abdelsalam, M. G., & Stern, R. J. (1996). Mapping Precambrian structures in the Sahara Desert with SIR-C/X-SAR radar: The Neoproterozoic Kerf Suture, NE Sudan. *Journal of Geophysical Research: Planets*, 101(E10), 23063–23076. <https://doi.org/10.1029/96JE01391>
- Abdelsalam, M. G., Stern, R. J., Copeland, P., Elfaki, E. M., Elhur, B., & Ibrahim, F. M. (1998). The Neoproterozoic Kerf Suture in Ne Sudan: Sinistral Transpression Along the Eastern Margin of West Gondwana. *https://Doi.Org/10.1086/516012*, 106(2), 133–147. <https://doi.org/10.1086/516012>
- Al-Djazouli, M. O., Elmorabiti, K., Zoheir, B., Rahimi, A., & Amellah, O. (2019). Use of Landsat-8 OLI data for delineating fracture systems in subsoil regions: implications for groundwater prospection in the Waddai area, eastern Chad. *Arabian Journal of Geosciences*, 12(7), 1–15. <https://doi.org/10.1007/S12517-019-4354-8/METRICS>
- Alexis, Plunder, Jérémie, & Melleton, Matthieu Chevillard, Guillaume Vic, I Ousman Al-Gadam, et al. . (2019). Tectonometamorphic evolution of the North Ouaddaï Massif (Am Zoer area, E. Chad). *Hal-02329009*, 2.
- B.R.G.M. (2010a). *Carte de favorabilité géologique à la présence d ' indices métalliques (Au - U - Cu - Pb - Zn - W - Sn)*. Echelle: 1/1500 000. Planche 8.
- B.R.G.M. (2010b). *Carte des formations géologiques*. Echelle 1/1500 000. Planche 1.
- Bessoles, B. & Trompette, R. (1980). *La chaîne panafricaine. Zone mobile d'Afrique centrale (partie sud) et zone soudanaise. Mémoire du Bureau de Recherches Géologiques et Minières, Orléans*.
- Chaussier, B.J., 1970. Carte minérale du Tchad. B.R.G.M. 2^e ed. 82p
- De Wit, M. J., Bowring, S., Buchwaldt, R., Dudas, F., Macphee, D., Tagne-Kamga, G., Dunn, N., Salet, A. M., & Nambatingar, D. (2021). Geochemical reconnaissance of the guéra and ouaddaï massifs in chad: Evolution of proterozoic crust in the central sahara shield. *South African Journal of Geology*, 124(2), 353–382. <https://doi.org/10.25131/SAJG.124.0048>
- Djerossem, F., Berger, J., Vanderhaeghe, O., Isseini, M., Ganne, J., & Zeh, A. (2020). Neoproterozoic magmatic evolution of the southern Ouaddaï Massif (Chad). *Bulletin de La Société Géologique de France*, 191(1), 34. <https://doi.org/10.1051/BSGF/2020032>
- Djerossem, F. N., Mbassa, B. J., Vanderhaeghe, O., & Gregoire, M. (2024). Comptes Rendus Géoscience. *Comptes Rendus. GÃ©oscience Ã¢fl Sciences de La PlanÃªte*, 356(G1), 231–248. <https://doi.org/10.5802/crgeos.282>

- Djerosseem Nenadji, F., 2018. Croissance et remobilisation crustales au Pan-Africain dans le sud du massif du Ouaddaï (Tchad). Thèse doct.Univ.Toulouse.303p
- Djerosseem, Nenadji, F., Rirabé, N., Ronang Baïsseмия, G., Ngarena Klamadji, M., & Hisseine Malik, M. (2024). Lineament and Lithological Mapping of Meta-Sediments and Granitoids of Goz-Beïda (Eastern Chad) Based on Semi-Automatic Processing of Landsat 8 Oli/Tirs Images. *Journal of Geosciences and Geomatics*, 12(4), 80–86. <https://doi.org/10.12691/JGG-12-4-1>
- Doumnang, Claude, M. J., Diondoh, M., Tekoum, L., & Rochette, P. (2024). Teleanalysis, structural mapping of t, geological and he southern zone of the Ttibesti metallogenic province (NortherN Chad). *International Journal of Applied Science and Research*, VOLUME 7(ISSUE 6 NOVEMBER – DECEMBER), 133–147.
- Doumnang, J.-C. (2006). *Géologie des formations néoprotérozoïques du Mayo Kebbi (Sud-Ouest du Tchad) : apport de la pétrologie et de la géochimie : implications sur la géodynamique au Panafricain / Theses.fr*. Orléans.
- Elsheikh, A., Abdelsalam, M. G., & Mickus, K. (2011). Geology and geophysics of the West Nubian Paleolake and the Northern Darfur Megalake (WNPL–NDML): Implication for groundwater resources in Darfur, northwestern Sudan. *Journal of African Earth Sciences*, 61(1), 82–93. <https://doi.org/10.1016/J.JAFREARSCI.2011.05.004>
- Faure, S. (2001). Analyse des linéaments géophysiques en relation avec les minéralisations en or et métaux de base de l’Abitibi. In *Rapport Projet CONSOREM (Vols. 2000-03A)*.
- Gsell, J. and Sonnet, J. (1962). *Prospection de re-connaissance sur la coupure de Niéré (feuille de Niéré N° ND 34 NE 0.80-E.8)*.
- Gsell J and Sonnet J., 1960. (1960). Carte géologique de reconnaissance au 1/500.000 et notice explicative sur la feuille Adre. Brazzaville. *BRGM*, 42.
- Hingue, N. V., Diondoh, M., Mbaigane, D., Claude, J., Lutian, A., Mbaïade, B., & Mbaihoudou, D. (2025). *Research article geological and structural mapping of the ouaddaï massif using landsat and radar data*.
- Hingue, N. V., Mbaigané, J. C. D., Diondoh, M., & Mbaihoudou, D. (2024). Petrography and Geochemistry of the Farchana-Hadjerhadid Granitoids (Ouaddaï Massif, Eastern Chad). *European Journal of Environment and Earth Sciences*, 5(4), 8–15. <https://doi.org/10.24018/EJGEO.2024.5.4.473>
- Ibinoof, A., M., Bumby, A. J., Liégeois, J.-P., Grantham, G. H., Armstrong, R., & Le Roux, P. (2021). *The Boundary Between the Saharan Metacraton and the Arabian Nubian Shield: Insight from Ediacaran Shoshonitic Granites of the Nuba Mountains (Sudan): U–Pb SHRIMP Zircon Dating*,

Geochemistry and Sr–Nd Isotope Constraints. 39–62. https://doi.org/10.1007/978-3-030-72995-0_2

Ibinoof, M. A., Bumby, A. J., Grantham, G. H., Abdelrahman, E. M., Eriksson, P. G., & le Roux, P. J. (2016). Geology, geochemistry and Sr–Nd constraints of selected metavolcanic rocks from the eastern boundary of the Saharan Metacraton, southern Sudan: A possible revision of the eastern boundary. *Precambrian Research*, 281, 566–584. <https://doi.org/10.1016/J.PRECAMRES.2016.06.010>

Isseini, M. (2011). *Croissance et différenciation crustales au Néoprotérozoïque : exemple du domaine panafricain du Mayo Kebbi au Sud-Ouest du Tchad* [Université Henri Poincaré - Nancy 1]. <https://hal.univ-lorraine.fr/tel-01746184>

Jean Pias. (1960). *Sols de la région Est du Tchad. plaines de Piedmont. massif du Ouaddai et de l'Ennedi.*;rapport. B.R/G.M.1960.336p

Kasser, Y. M. (1995). *Evolution précambrienne de la région du Mayo Kebbi (tchad), un segment de la chaîne pan-africaine* [dohttps://bibliotheques.mnhn.fr/medias/doc/Exploitation/horizon/472164/evolution-precambrienne-de-la-region-du-mayo-kebbi-tchad-un-segment-de-la-chaîne-pan-africaine](https://bibliotheques.mnhn.fr/medias/doc/Exploitation/horizon/472164/evolution-precambrienne-de-la-region-du-mayo-kebbi-tchad-un-segment-de-la-chaîne-pan-africaine)

Kusnir, I. (1989). *aperçu sur la géologie, les ressources minérales et en eau du Tchad*.

Kusnir, I. (1995). *Géologie, ressources minérales et ressources en eau du Tchad ; Travaux. centre national de recherche*.217P

Liégeois, Jean, P., Abdelsalam, G., M., Ennih, N., & Ouabadi, A. (2013). Metacraton: Nature, genesis and behavior. *Gondwana Research*, 23(1), 220–237. <https://doi.org/10.1016/J.GR.2012.02.016>

Liégeois, Paul, J., Abdelsalam, M. G., Ennih, N., & Ouabadi, A. (2013). Metacraton: Nature, genesis and behavior. *Gondwana Research*, 23(1), 220–237. <https://doi.org/10.1016/J.GR.2012.02.016>

Malik, M. H., NgonNgon, G. F., Vishiti, A., Mayer, A.-S. A., Isseini, M., Djerosse, F., & Al-Gadam, I. O. (2024). Petrography and mineral microchemical signature of lode gold mineralization in Goz-Beida, southern Ouaddaï massif, eastern Chad. *Arabian Journal of Geosciences* 2024 17:7, 17(7), 1–19. <https://doi.org/10.1007/S12517-024-12011-5>

Mbagedje, D. (2015). *Métallogénie de l'or et de l'uranium dans le cadre de la croissance et de la différenciation de la croûte au Néoprotérozoïque : exemple du massif du Mayo-Kebbi (Tchad) dans la Ceinture Orogénique d'Afrique Centrale* [Université de Lorraine]. <https://hal.univ-lorraine.fr/tel-01751338>

Mbaiade, B. (2023). *Etude géologique de la localité de Goz-Beida (région est du Tchad) : apport de la*

téledétection, la pétrographie et la structurale.Mém.mast.Univ.N'gaoudéré.90p

Mbaitoudji, M. . (1984). *Lois de répartition, hypothèse de pronostics et méthodologie de la recherche des gisements de minéraux utiles solides dans le territoire de la République du Tchad*.rapport. 14p

Mestraud, J. P. (1964). Carte géologique de la République Centrafricaine à l'échelle du 1/1.500.000. *BRGM*.

Michael, G. houahdibe. (2017). *Contribution à l'étude pétrographique et structurale du secteur Nord de Goz-Beïda (Massif du Ouaddaï-Tchad)*.Mém.mast.univ.N'gaoundéré.85p

Oussama, M. A. T. (2023). *Etudes pétrographique et structurale des formations magmatiques et métamorphiques du massif du Ouaddaï (Axe Abéché – Adré)*.Mém.Mast.univ.N'djaména.46p

Pazeu, Y. G. (2018). *Caractéristiques, pétrographiques, structurales et géochimiques du socle précambrien de la localité d'Am Zoer : massif du Ouaddaï (Est du TCHAD)*.Mém.Mast.Univ.N'gaoudéré.89p

Penaye, J., Kröner, A., Toteu, S. F., Van Schmus, W. R., & Doumnang, J. C. (2006). Evolution of the Mayo Kebbi region as revealed by zircon dating: An early (ca. 740 Ma) Pan-African magmatic arc in southwestern Chad. *Journal of African Earth Sciences*, 44(4–5), 530–542. <https://doi.org/10.1016/J.JAFREARSCI.2005.11.018>

Richards, J. P. (2000). Lineaments Revisited. *Society of Economic Geologists*, 42, 1–20. <https://doi.org/10.5382/SEGNEWS.2000-42.FEA>

Scanvic, J. Y. (1986). *Téledétection aérospatiale et informations géologiques. Manuels et Méthodes. Éditions* (Éditions 2d).

Schneider, J. L. (2001). *Géologie, Archéologie, Hydrogéologie de la République du Tchad.. Carte de valorisation des eaux souterraines de la République du Tchad, 1/1500000, Direction de l'hydraulique, N'djamena*. <https://www.sciepub.com/reference/372321>

Schneider J.L., & Wolff, J. . (1992). Carte géologique et cartes hydrogéologiques à 1/1 500 000 de la République du Tchad. Mémoire explicatif. In *Documents - B.R.G.M.* Bureau de recherches géologiques et minières.

Shellnutt, Gregory J., Pham, N. H. T., Yeh, M. W., & Lee, T. Y. (2020). Two series of Ediacaran collision-related granites in the Guéra Massif, South-Central Chad: Tectonomagmatic constraints on the terminal collision of the eastern Central African Orogenic Belt. *Precambrian Research*, 347, 105823. <https://doi.org/10.1016/J.PRECAMRES.2020.105823>

Shellnutt, J. G., Pham, N. H. T., Denyszyn, S. W., Yeh, M. W., & Lee, T. Y. (2017). Timing of

collisional and post-collisional Pan-African Orogeny silicic magmatism in south-central Chad. *Precambrian Research*, 301, 113–123. <https://doi.org/10.1016/J.PRECAMRES.2017.08.021>

Shellnutt, J. G., Yeh, M. W., Lee, T. Y., Iizuka, Y., Pham, N. H. T., & Yang, C. C. (2018). The origin of Late Ediacaran post-collisional granites near the Chad Lineament, Saharan Metacraton, South-Central Chad. *Lithos*, 304–307, 450–467. <https://doi.org/10.1016/J.LITHOS.2018.02.020>

Stern, R. J., & Abdelsalam, M. G. (1998). Formation of juvenile continental crust in the Arabian-Nubian shield: Evidence from granitic rocks of the Nakasib suture, NE Sudan. *International Journal of Earth Sciences*, 87(1), 150–160.

Théodore, Yao, K., Olivier, & Fouché-Grobla, Marie-Solange Yéi Oga, V. T. A. (2012). Extraction de linéaments structuraux à partir d'images satellitaires, et estimation des biais induits, en milieu desocle précambrien métamorphisé. *Teledetection*, 10 (4), pp.161-178. {hal-01948904}.

Wolff, J. P. (1964). *Carte géologique de la République du Tchad au 1/1500000, BRGM, Paris.*

World bank group. (2023). *Tchad Rapport diagnostique du secteur minier.*Rapport. 131p